

Title: To what extent have changes in channel capacity contributed to flood hazard trends in England and Wales?

Louise J. Slater*

School of Geography, Queen Mary, University of London, London, UK

Now at IIHR-Hydroscience & Engineering, The University of Iowa, Iowa City, IA, 52242, USA

**Correspondence to: L. J. Slater. E-mail: louise-slater@uiowa.edu*

This article has been accepted for publication and undergone full peer review but has not been through the copyediting, typesetting, pagination and proofreading process, which may lead to differences between this version and the Version of Record. Please cite this article as doi: 10.1002/esp.3927

ABSTRACT

The frequency of floods has been projected to increase across Europe in the coming decades due to extreme weather events. However, our understanding of how flood frequency is affected by geomorphic changes in river channel capacity remains limited. This paper seeks to quantify the influence of trends in channel capacity on flood hazards. Measuring and predicting the effect of geomorphic changes on freshwater flooding is essential to mitigate the potential effects of major floods through informed planning and response. Hydrometric records from 41 stream gauging stations were used to measure trends in the flood stage (i.e. water surface elevation) frequency above the 1% annual exceedance threshold. The hydrologic and geomorphic components of flood hazard were quantified separately to determine their contribution to the total trend in flood stage frequency. Trends in cross-sectional flow area and mean flow velocity were also investigated at the same flood stage threshold. Results showed that a 10% decrease (or increase) in the channel capacity would result in an increase (or decrease) in the flood frequency of approximately 1.5 days per year on average across these 41 sites. Widespread increases in the flood hazard frequency were amplified through both hydrologic and geomorphic effects. These findings suggest that overlooking the potential influence of changing channel capacity on flooding may be hazardous. Better understanding and quantifying the influence of geomorphic trends on flood hazard will provide key insight for managers and engineers into the driving mechanisms of fluvial flooding over relatively short timescales.

KEY WORDS: Flood hazard, England and Wales, Trends, Channel capacity, Hydrometric data.

INTRODUCTION

Catastrophic fluvial floods are often caused by exceptionally heavy and prolonged rainfall linked to atmospheric circulation patterns (e.g. Slingo *et al.*, 2014, Huntingford, 2014). The magnitude and frequency of such events is driven by changes in climate (Wilby *et al.*, 2008, Pall *et al.*, 2011), as well as by shifts in land use and land management (e.g. Wheeler and Evans 2009, Kjeldsen, 2010, Pattison and Lane, 2012, Prodoscimi *et al.*, 2015) and socio-economic policies and practices (Hall *et al.*, 2003). Recently, a 'new' driver has also been gaining increasing attention: the influence of geomorphic changes in river channel capacity on flood extent/duration (Lane *et al.*, 2007, Neuhold *et al.*, 2009), and frequency (Slater *et al.*, 2015).

Alluvial river channels have erodible boundaries that are self-formed by the transport of sediment-laden flow, and thus they adjust their morphology over time to reflect the average volumes of sediment and water that are supplied to them from the upstream basin (Leopold and Maddock, 1953; Schumm and Lichty, 1965). Because of the dynamic nature of river systems, changes in the flow frequency, sediment supply, and vegetation can alter channel geometry (i.e. the width, depth, and velocity of cross-sectional flow) and therefore the capacity of river channels to contain flood flows. Freshwater flooding occurs when the capacity of a river channel to hold the incoming volume of water per unit time is exceeded. Once the bankfull channel capacity is reached, the streamflow spills out into the floodplain. A change in the frequency and areal extent of flooding can therefore be caused by one of two factors: a change in the frequency of high flows (the "flow frequency effect"), and/or a change in the capacity of the channel to contain floods (the "channel capacity effect") (Slater *et al.*, 2015).

The aim of this paper is to assess the historical contribution of geomorphic trends in channel capacity to the frequency of flooding across England and Wales. Channel capacity and flow frequency 'effects' on flood hazard frequency are measured separately to assess their influence on flooding and to evaluate whether they are increasing/decreasing flood frequency in unison, or counterbalancing one another. This understanding will provide better insight for managers and engineers into the driving mechanisms of fluvial flooding over relatively short (annual to decadal) timescales.

CONTEXT, DATA AND METHODS

Flood hazard in England and Wales

Flooding is the most common and the most expensive natural hazard in the British Isles. The cost of flooding and of managing floods has been estimated at around £2.2 billion per year (Evans *et al.*, 2004), and has been projected to increase approximately twentyfold in England and Wales under future scenarios and assuming the case of the highest projected economic growth (Hall *et al.*, 2005). If no action is taken to limit emissions, an estimated 2.3 to 3.6 million people in England and Wales are expected to be at some risk of flooding by the 2080s (Evans *et al.*, 2004), with the majority of costs incurred by households and businesses (Chatterton *et al.*, 2010). It is therefore essential that we understand the different drivers of flooding so that we can mitigate their potential effects through informed planning and response.

The 2014 UK winter floods gave rise to a national controversy on the influence of channel capacity on flood hazard. The public debated at length whether the flooding had been exacerbated by a build-up of silt due to inadequate dredging and over-intensive agricultural practices (Thorne, 2014). However, it still remains unclear to what extent changes in channel/network capacity have altered the spatial extent, frequency, and duration of flooding. Research conducted in the late 1980s revealed that geomorphic channel adjustments were widespread in England and Wales. Brookes (1987) observed channel morphology downstream from 46 channelization works through a variety of field survey, mapping, and photographic methods, and found that channels had enlarged due to increased flood flows and stream velocities that scoured the river banks and beds. Channel changes measured between 1870 and 1950 by Hooke and Redmond (1989) also indicated extensive instability in over a third of rivers in upland England. Yet the effects of such changes in channel morphology on flood hazards have received very little attention in the literature.

Historic approaches for quantifying geomorphic effects on flood hazard frequency

A handful of modelling studies have investigated the influence of geomorphic change on flood inundation depths. Lane *et al.* (2007) used hydrodynamic modelling of a reach of the River Wharfe and found that aggradation of the gravel-bed was responsible for about half of the short-term increase in flood extent. Simulations of flow and sediment

transport scenarios during flood events revealed that incorporating changes in river bed elevation (Neuhold *et al.*, 2009), or changes in channel capacity (Fewtrell *et al.*, 2011) in the models was necessary for accurately measuring changes in flood inundation depths and associated uncertainties. Wong *et al.* (2014), on the contrary, found that changes in riverbed erosion had little effect on inundation depth during a flood event, but recognised that their model did not incorporate lateral changes in river width or in-channel sedimentation – i.e. the two principal drivers of increasing flood hazard from channel capacity changes (e.g. Raven *et al.*, 2009). Few models have attempted to incorporate the feedback effects of changing channel morphology, sediment, and vegetation cover on flood flows, as it is challenging to correctly reproduce erosion and deposition patterns (Hooke *et al.*, 2005).

Empirical approaches for estimating changes in channel capacity and their effects on flood hazard frequency are mostly based on a method termed ‘equal discharge’ analysis by Gilbert (1917) and later ‘specific gauge analysis’ by Blench (1969). The method consists in plotting the water levels associated with a reference (fixed) discharge over time (e.g. Pinter and Heine, 2005). If the stage decreases over time, then the channel capacity must have increased (through bed degradation, widening, and/or decreased roughness), while an increase indicates that the channel capacity must have decreased (through aggradation, narrowing, and/or increased roughness). This approach has been used successfully to determine how changes in channel capacity alter flood stage frequency (e.g. Biedenharn and Watson, 1997, Stover and Montgomery, 2001). Marsh and Harvey (2012) used a similar approach to show that increasing channel capacity decreased the annual maximum flood levels on the Thames. To understand how such changes in channel capacity actually alter the frequency of flood flows, Slater *et al.* (2015) developed a statistical approach combining gauging transect measurements with daily flow records in over 400 sites across the USA. Here, we go one step further by showing how the flow frequency effect and the channel capacity effect combine statistically to produce the overall change in flood hazard frequency.

Using hydrometric data to quantify channel capacity effects on flood hazard frequency

Until recently, our ability to examine geomorphic changes in large numbers of river channels was hindered by the lack of data spanning vast geographic areas and long time-periods. In the last few years, however, many environmental agencies have made

their historical databases of hydrometric measurements freely accessible to the public. Across England and Wales, there is a dense network of over 600 gauging stations (Lamb *et al.*, 2003). At these stations, manual transect measurements are made to calculate the volume of discharge that is carried within the stream cross-section at any given point in time as:

$$Q = A \cdot V \quad (1)$$

where A is the area and V is the average velocity of the cross-sectional streamflow. These individual fluvial transect measurements are made repeatedly over time for different water levels (stage, sometimes also referred to as the gauge height), so that a rating curve can be developed, relating the discharge to the stage. These rating curves allow water managers to estimate the discharge at the gauge based on a simple reading of the water level. As alluvial channels adjust their form over time in response to sudden or incremental flood events, past rating curves are rendered inaccurate and must be updated with new measurements (Carter and Davidian, 1968). Once the 'old' hydrometric measurements have served their purpose, they are typically filed away in an historical database. However, instead of simply archiving these data once they become obsolete, we can use them to obtain valuable insight into the geomorphic changes that occur in river channels. Provided one establishes rigorous filtering procedures, the streamflow measurements that are made repeatedly in one location over time can serve to estimate changes in the channel geometry (i.e. the width, mean depth, and mean velocity of the cross-sectional flow), and in the capacity of the channel cross-section to contain flood flows. Such statistical analyses can be automated across a broad range of climatic and geologic contexts (Slater and Singer, 2013, Slater *et al.*, 2015).

For this study, complete historical time-series of river channel transect measurements of cross-sectional flow were requested from the Environment Agency (EA, national.requests@environment-agency.gov.uk) and from Natural Resources Wales (NRW, accesstoinformationteam@naturalresourceswales.gov.uk) for all 'velocity-area' stream gauges where the river channel cross-section is able to adjust freely over time (i.e., not impaired by the presence of a major structural control). These transect measurements are provided by EA and NRW in spreadsheets which contain 19 attributes (columns) including the Site Name, Number, Grid Reference, River, Status, Quality, Date and Time, Stage start and end time, Mean stage (m), Flow (m^3/s), Width of River (m), Gauging Deviation (%), Cross-section of the flow area (m^2), Mean Velocity

of the flow (m/s), Wetted Perimeter (m), Mean Depth (m), Measurement Type, Calculation Method, Team conducting the measurement, Parameter, and any Remarks for each measured transect (row).

One of the principal challenges of using stream transect measurements to measure temporal trends in channel geometry is that the exact location where streamflow gaugings are made is not always recorded. However, it is critical that trends in channel geometry are measured in one consistent cross-sectional location over time. While most measurements tend to be made in a similar location near the gauge, the exact location chosen by the operator may vary depending on the instrument used, the presence of obstructions in the river such as weed growth or debris, the operator's knowledge of the instruments or of the site, and the time of year or meteorological conditions, since low and high flows are not always made in the same location (N. Everard, pers. comm.).

The 'Measurement Type' and 'Remarks' attributes in the data spreadsheet provide an indication of the instrument used to measure the flow and the location where the measurement was made (off cableway, approximate distance up or downstream from the gauge, etc.). These qualitative descriptions vary considerably and thus it is problematic to define an 'automatic' filtering criterion. From reading many of the comments in the "Remarks" column and multiple discussions with EA and NRW field officers, it appears that the most consistent measurement location, by far, is the cableway. Therefore, the individual transect measurements were filtered to retain only measurements made specifically at the cableway by conducting an automated search for the three letter string "cab" (or CAB) in the column "Remarks". This filtering step means that any trends in the channel capacity will be measured consistently in one given location over time (**Figure 1**).

Preliminary filtering steps were as follows. Any transect measurement (i.e. one row in the spreadsheet corresponding to one cross-sectional measurement of the channel cross-section at one date and time) missing the date or stage was entirely removed, as were any measurements that contained missing, zero, or negative values of discharge. The mean flow velocity was provided for the majority of transect measurements, but not the flow area. Therefore, because discharge is calculated as the product of flow area and mean flow velocity as in equation 1, the cross-sectional flow area values were back-calculated as the ratio of discharge to flow velocity. Following these filtering steps, only the sites with a minimum of 10 historical cross-sectional transect measurements

made *at the cableway* were retained; on average, the final gauging sites have 116 cross-sectional flow measurements each. The time period spanned by each transect measurement time series was used as the baseline time-period for the study (for computing channel capacity, flow frequency, and flood stage frequency trends) at each gauging station (see **Tables 1-3** in the supplementary materials). The median record length of channel measurements is 29 years.

Daily stage and streamflow data

Mean daily stage time-series were obtained for the sites satisfying the above filtering criteria from the EA and NRW via email request. All of the sites are active National River Flow Archive (NRFA) gauging stations, so the mean daily streamflow data were downloaded from the NRFA website using the 'nrfa' package (Vitolo and Fry, 2014) in the open-source software R. Both the historic mean daily stage time-series and the mean daily discharge time-series were tailored to cover the same time period as the channel transect measurements, so they could not extend before, or after, the year in which the first and last channel measurements were recorded at each site.

While hydrologic trend studies typically use at least 20 years of data, the emphasis of this paper is on dissociating the contribution of flow frequency and channel capacity to the flood stage frequency trends over short timescales that are of relevance to flood managers (i.e., where infilling sediment, debris, or weed can substantially modify the channel capacity). Additionally, only few stations have complete long-term overlapping data for channel transect measurements, daily stage, and daily discharge. For all of these reasons, it was deemed necessary to relax some of the filtering criteria, and retain all gauging records with a length of at least 10 complete years of daily stage and discharge data. The minimum time series length was 11 years, but the mean length was 26 years. Plots of all data for each site are provided in the supplementary materials.

The final selection of 41 gauging sites (**Figure 2**) reflects the regions where the EA and NRW provided most data and the locations with sufficient discharge, stage, and transect measurements after all of the filtering steps. The sites are located across the following hydrometric regions and areas: Midlands (9 Central, 2 East, 6 West), North East (8 Yorkshire, 3 North East), North West (2 South), South East (1 West Thames), South West (6 Devon and Cornwall), and Wales (1 North, 3 South West).

Remarks concerning the data

First and foremost, readers will note the inherent connection between the flow, stage, and channel transect records at each site, since daily discharge time series are derived from the stage-discharge rating curve (obtained from the transect measurements at each gauging station). What makes this analysis possible is the fact that the stage/discharge time series are continually adjusted based on the most recent gauging transects. Therefore the transect measurements can be used in residual analysis to understand how the channel capacity has changed, and the stage/discharge time series are also an accurate representation of the trend in stage/discharge over time.

Second, the transect gauging measurements used in this study are open-channel measurements which tend to be within $\pm 5\%$ uncertainty at the 95% confidence level, according to the standard error of the mean relation (SMR) statistic (Herschy, 1995). However, the accuracy of these measurements may vary depending on a variety of factors including survey errors, algae, aggradation/degradation of the bed, etc. Because of this potential source of error, trend detection methods (described in the methodology) used a weighting procedure to minimize the influence of error and outliers in the data.

Third, the measurements that are used here to quantify changes in channel capacity are gauging *transects*, so they only inform us about geometric changes within one specific channel cross-section. Changes at the scale of the transect may or may not be representative of changes occurring within the entire reach. Unfortunately, hydrometric measurements made at the scale of the reach are relatively rare, and transect data are the only spatial scale for which such long time-series and precise/accurate measurements of streamflow exist. In some ways, the poor spatial resolution of gauging data is offset by their high temporal resolution.

Lastly, this paper does not seek to distinguish sites with natural flow conditions (5 of the studied sites) from those with modified flow conditions (the remaining 36 sites). As noted in previous work (Slater and Singer, 2013, Slater *et al.*, 2015), changes in channel geometry at any given location can be caused by a mix of climatic and anthropogenic influences on the hydrologic regime as well as changes to sediment delivery within the catchment. It can be challenging to disentangle the causes of changes in channel capacity and flow frequency. Therefore, this paper aims to quantify the magnitude of geomorphic vs. hydrologic influences on flood hazard frequency rather than to pinpoint what the causes of those changes may be.

Methods overview

The methodology can be summarised as follows, with each of the sections below providing further details. First, the ‘flood stage’ threshold was defined as the 99th percentile of the stage time-series, G_{99} , and the flood stage frequency trend calculated using a peak-over-threshold (POT) approach. The time-averaged “channel capacity” (discharge), flow area, and mean flow velocity at flood stage were then determined at G_{99} (\overline{Q}_{99} , \overline{A}_{99} and \overline{V}_{99}). The channel capacity, flow area, and flow velocity were also estimated at G_{99} at each point in time when a gauging measurement was made (\hat{Q} , \hat{A} and \hat{V}). These values were used to compute the trend in channel capacity, flow area, and flow velocity at flood stage. Separately, an exceedance frequency curve was computed using the mean daily flow values, and used to calculate the historic exceedance frequency (F) of channel capacity at each point in time (\hat{Q}). From there, the “channel capacity effect on flood hazard” was calculated as the trend in flood hazard frequency that arose from changes in the channel capacity exclusively (while holding the flow frequency distribution constant). Lastly, the “flow frequency effect on flood hazard” was computed as the trend in flood hazard frequency that arose from changes in the flow frequency distribution (while holding the channel capacity constant). The same POT approach was used to calculate the flow frequency effect as for stage. The sum of channel capacity and flow frequency effects should correspond to the flood stage frequency trend. The trend-detection methods for channel capacity and flow frequency are the same as those used in Slater *et al.* (2015) and are recalled here for clarity. The detection of trends in flood stage frequency and the evaluation of channel capacity and flow frequency effects on flood hazard as components of the trend in flood stage frequency, however, is new.

Trend in flood stage frequency

The threshold at which to evaluate trends in the channel capacity and flow frequency was set as the 99th percentile of the total mean daily stage distribution (G_{99}) over the reference period (**Figure 3**). G_{99} , hereafter referred to as the “flood stage”, is the 1% annual exceedance level, and is used as the common threshold for computing trends in flood stage frequency, channel capacity effects and flow frequency effects (**Figures 4-5**). Importantly, the channel capacity is *not* defined here as the capacity of the channel at bankfull elevation. This is a crucial element of the method: using a fixed flood threshold (G_{99}) rather than the bankfull elevation (which may change over time) allows

us to dissociate the different components of flood hazard frequency (hydrologic vs geomorphic) and investigate what is driving the changes in the highest flood flows *at that level*.

The trend in flood stage frequency was computed using a POT approach. POT methods are commonly used to measure trends in the frequency of extreme flows (e.g. Naden, 1992, Lang *et al.*, 1999). For each year, the total number of days exceeding G_{99} was computed (number of days per year where $G > G_{99}$), and a trend of mean unbiased exponential form was fit to the annual totals (**Figure 4B**), of the form:

$$\frac{EF}{\text{mean}(EF)} = \frac{\exp(r\Delta t)}{\text{mean}(\exp(r\Delta t))} \quad (2)$$

where $\text{mean}(EF)$ is the mean of the observed annual calculated exceedance frequencies, r is the fractional change in flow frequency per unit of time, and $\Delta t = \text{date} - \text{mean}(\text{date})$, where $\text{mean}(\text{date})$ is the midpoint of the time series. If Δt is expressed in decades, then 100 times the coefficient r yields the rate of change in flood-stage flow frequency in percent per decade.

Time-averaged discharge (“channel capacity”), flow area, and mean flow velocity at flood stage (\overline{Q}_{99} , \overline{A}_{99} , \overline{V}_{99})

To quantify the average discharge, flow area, and mean flow velocity of the channel cross-section at G_{99} , Locally weighted scatterplot smoothing (Loess) curves (Cleveland, 1979) were fit to the relationships relating stage to the log-transformed cross-sectional discharge measurements using the Loess library from the R “stats” package (Ripley, 2014). The α fitting parameter, which determines the proportion of data that is used to fit each polynomial at each point in the curve, ranges from 0 to 1, and was left at the default value of 0.75, which produced a good fit to the data (all of the plotted curves are shown in the Supplementary materials). Q was extracted at the point where G_{99} intersects the curve. This fixed value, termed \overline{Q}_{99} (m^3/s), represents the average flow at G_{99} over the time period when the measurements were made, or in other terms the time-averaged channel capacity at the 99th percentile of the stage distribution. Eight extreme outliers were detected and considered to be measurement errors. These points were removed (0.002% of the dataset) because they strongly perturbed the Loess fit through the data points. \overline{Q}_{99} ranged from 3.5 m^3/s for the River Rea at Calthorpe Park to 330 m^3/s for the River Wye at Belmont, with a mean channel size of

63 m³/s across all channels (**Table 1** in the Supplementary materials). Drainage area ranges from 74 km² for the Rea to 3072 km² for the Trent at Drakelow.

A subset of 34 sites was created specifically for the gauging stations that also had mean cross-sectional velocity and cross-sectional flow area measurements (**Figure 2**, white inner circles). The time-averaged mean flow velocity \overline{V}_{99} , and the time-averaged flow area \overline{A}_{99} , were computed using the same procedure as for discharge.

Trend in discharge, flow area and mean flow velocity at flood stage

Trends in channel capacity (discharge), flow area and mean flow velocity of the channel cross section can be calculated using residuals from the Loess curve. A similar approach has been used in the past to observe changes in channel capacity (James, 1997, 1991). The procedure corrects for differences in G without assuming that the relationship between Q , A , or V , and G has any particular functional form (Helsel and Hirsch, 1993). The validity of the method requires a good fit of the regression relationship and approximate equivalence of the residuals for all levels of stage. The regression residuals (i.e. the observed minus the predicted values of the relationship, indicated by a hat above the variable name and the subscript ϵ) were computed as:

$$\ln(\hat{\alpha}_{\epsilon i}) = \ln(\alpha_i) - \ln(\overline{\alpha_i}) \quad (3)$$

where $\ln(\alpha_i)$ are the natural logarithms of the observed transect measurements of discharge, flow area, or flow velocity, and $\ln(\overline{\alpha_i})$ are the estimated values on the Loess curve (i.e., they represent time-averaged values of $\ln(Q)$, $\ln(A)$, or $\ln(V)$) (**Figure 5A** for discharge, **Figure 6A** for flow velocity and **Figure 6C** for flow area). For example, a negative discharge residual (point below the Loess curve) would indicate a smaller value of “channel capacity” for that elevation compared to the average channel capacity over the entire period. The discharge, flow area, and mean flow velocity of the channel cross-section were then estimated at G_{99} at different points in time by adding the value of each residual to the average discharge (**Figures 5A, 6A, 6C**) as:

$$\ln(\hat{\alpha}) = \ln(\overline{\alpha_{99}}) + \ln(\hat{\alpha}_{\epsilon i}) \quad (4)$$

where the resulting values of $\ln(\hat{\alpha})$ are the logarithmic estimates of Q , A , or V , that would be required at the time of each manual field measurement to attain G_{99} . Since the estimated values of cross-sectional discharge, flow area, and mean flow velocity

are likely to display some scatter due to minor measurement errors (unlike the trend in flow frequency / flood stage frequency, where there is less error in counting the number of days above a threshold), an iteratively reweighted least squares (IRLS) procedure was used with a Cauchy weighting function (Holland and Welsch, 1977, as applied in Slater *et al.* (2015)) to downweight the influence of outliers and produce a trend that passes through the values, as:

$$w_i = \frac{1}{1 + \frac{a_i^2}{3.536MAR}} \quad (5)$$

where a_i is the residual corresponding to an individual point, and MAR is the median absolute residual. The trend in estimated values of $\hat{\alpha}$ is computed similarly to equation 2, using the exponential unbiased mean form:

$$\frac{\hat{\alpha}_{\varepsilon_i}}{wt.mean(\hat{\alpha}_{\varepsilon_i})} = \frac{\exp(r\Delta t)}{wt.mean(\exp(r\Delta t))} \quad (6)$$

where $\hat{\alpha}_{\varepsilon_i}$ is the estimate of \hat{Q} corresponding to an individual point, $wt.mean(\hat{\alpha}_{\varepsilon_i})$ is the weighted mean of the estimates of $\hat{\alpha}_{\varepsilon_i}$ using the IRLS weights for each point; r is the fractional change in $\hat{\alpha}_{\varepsilon_i}$ per unit of time; and $\Delta t = \text{date} - \text{mean}(\text{date})$, as in equation 2. Because the outliers are down-weighted, the means must be weighted (i.e. calculated based on the weights that are given to each point in the fit) and updated for each iteration of the IRLS (**Figure 5B** for discharge, **Figure 6B** for flow velocity, and **Figure 6D** for flow area). To allow the comparison among channels of varying size, the trends in discharge, flow velocity and flow area were computed in percent per decade (in equation 6, r times 100, with Δt expressed in decades). Trends are also expressed in their dimensional form (in m^3/s , m^2 , or m per decade). See **Tables 2 and 3** in the supplementary materials for further information on trend length and magnitude at individual sites.

Channel capacity effect on flood hazard

To compute the channel capacity effect on flood hazard frequency, the mean daily discharge data (previously tailored to overlap with the transect measurements), were used to compute an exceedance curve (**Figure 5C**) relating the exceedance frequency F to Q as:

$$F_i = 365.25 \cdot \frac{\text{rank}(Q)_i}{(n+1)} \quad (7)$$

where $\text{rank}(Q)_i$ is the rank of each mean daily streamflow value, in descending order, and n is the total number of mean daily streamflow values over the entire period. The values were plotted in log terms (**Figure 5C**). The estimated values of channel capacity at G_{99} in their log form $\ln(\hat{Q})$ were pinpointed on the exceedance curve, and the corresponding exceedance frequencies were extracted. The exceedance curves were “cropped” to within ± 0.2 log units from the minimum and maximum $\ln(\hat{Q})$ values, to obtain a close fit of the Loess curve (because the $\ln(\hat{Q})$ values are often located at the tail end of the exceedance frequency distribution). Finally, the channel capacity effect was computed from these extracted recurrence values, using the same curve fit as equation 6, to downweight the influence of any outliers or minor errors in the data (**Figure 5D**).

Flow frequency effect on flood hazard

To compute the flow frequency effect, the daily discharge data were used to count the number of days per year where discharge exceeded \overline{Q}_{99} (the average channel capacity at G_{99}). This approach measures changes in the flow frequency *assuming a constant channel capacity over time*. In other terms, the flow frequency effect is measured as the trend in flood hazard frequency that would have arisen from shifts in the flow frequency distribution exclusively, if channel capacity had not changed. Only ‘complete’ years of data, with at least 350 measurements per annum, were retained. The same trend fit as for flood stage frequency (equation 2) was then fit to the annual POT values (**Figure 4**).

Total flood hazard frequency: the sum of both effects

It is possible to verify how accurately the total change in flood hazard frequency corresponds to the sum of channel capacity and flow frequency effects by calculating the discrepancy between measured trends as follows:

$$\text{Discrepancy} = \frac{|(\Delta_C + \Delta_F - \Delta_S)|}{\sqrt{\sigma_C^2 + \sigma_F^2 + \sigma_S^2}} \quad (8)$$

where Δ_C , Δ_F and Δ_S are the channel capacity effect on flood frequency, the flow frequency effect on flood frequency, and the trend in flood stage frequency,

respectively, in units of percent per decade; σ_C , σ_F , and σ_S are the standard errors of those same trends, also in units of percent per decade.

RESULTS

Hydrologic and geomorphic trends

How do changes in river channel capacity alter the frequency of floods above the 1% annual exceedance threshold (G_{99})? On average, across the 41 channel cross-sections, a 10% decrease in the channel capacity corresponded to an increase in the flood hazard frequency of approximately 1.5 day/year. Similarly, a 10% increase in the channel capacity decreased the frequency of flooding by approximately 1.5 days/year on average (**Figure 7**). This relationship between the trend in channel capacity and the trend in flood hazard frequency was comparable for both small and large channels (**Figure 7**) due to the similarity of exceedance curve slopes across the studied sites (see figures in the Supplementary materials).

Changes in channel capacity were then split into positive vs. negative trends to assess any differences in the average magnitudes of increasing vs. decreasing capacity, and to visualise the spatial distribution of these changes and their effects on flood hazard frequency across England and Wales. Decreases in the river channel capacity produced increases in flood hazard frequency of +7%/decade on average (24 sites, median: $-1.1\text{m}^3/\text{s}/\text{decade}$). Increases in channel capacity were smaller, reducing flooding by -3%/decade on average (17 sites, $+0.5\text{m}^3/\text{s}/\text{decade}$) (**Figure 8A**). These capacity trends were significant at almost half of all sites (-13/+12%/decade), and were in keeping with the trend magnitudes that were detected at gauging stations across the United States (Slater *et al.*, 2015).

Flow frequency effects on flood hazard were typically several times larger than the geomorphic effects. Median decreases/increases in flood hazard frequency were of -8/+17% per decade across 7 and 34 sites, respectively (**Figure 8B**). Note that these measured short-term changes in flow frequency are not necessarily representative of long-term climatic trends, which have been mostly insignificant in England and Wales for the last 80-120 years (Robson, 2002, Simpson and Jones, 2014). Significant flow frequency effects were present at far fewer sites than the significant channel capacity effects, but were much larger, at -123/+47% per decade (only 1 and 8 sites respectively). This relatively low proportion of statistically significant flow frequency

effects may be explained by the strong inter-annual variability in peak flows, so much stronger trends are needed (in comparison with the channel capacity effects) before they become statistically significant (Wilby, 2006). While only 3 sites (7%) displayed both effects at a significant level, the flow frequency effects on flood hazard were greater than the channel capacity effects at the vast majority (78%) of sites.

Figure 9 shows the spatial distribution of flood hazard frequency increases (red) and decreases (blue) from both effects across England and Wales. Channel capacity effects were mostly positive (58%), indicating increases in flood hazard from decreasing channel capacity (**Figure 9A**), although this proportion was not significant by sign test. Flow frequency effects, more remarkably, were significantly positive across the 41 sites ($p\text{-value} < 0.001$, 83% of sites, **Figure 9B**).

Interaction between channel capacity and flow frequency

Comparing geomorphic and hydrologic effects within every river channel cross-section reveals that these effects have the same sign (both increasing / both decreasing flood hazard) in almost half of the channels (19/41). In other terms, the trend in flood hazard frequency, whether positive or negative, is amplified by geomorphic changes at the 19 sites. These “additive” effects, which are displayed as black triangles in **Figure 10A**, are overwhelmingly positive (18/19 sites, or 95%), thus exacerbate the increase in flood hazard frequency.

For comparison, the total trend in flood hazard frequency resulting from *both* hydrologic and geomorphic changes can also be measured by the trend in flood stage frequency above a peak threshold, which is set here as the 99th percentile of the flow distribution (i.e., a flow frequency of 1% per year, or 3.65 days per year). The trends in flood stage frequency also reveal increasing flood hazard in a significant majority of channels (78% of sites, $p < 0.001$) (**Figure 10B**). Median increases/decreases in flood stage frequency are clearly larger than those produced by either of the two effects taken separately, at $-19\%/+31\%$ per decade (9 and 32 sites respectively, **Figure 8C**).

To assess how well the sum of computed channel capacity and flow frequency effects corresponds to the trend in flood stage frequency, the discrepancy was calculated following equation 8, and the relationship between both effects is shown in **Figure 11**. The median discrepancy for this dataset is 0.45, with only 2 sites (<5% of the dataset) exceeding a discrepancy of 2. These results suggest that the trends in flood stage frequency can indeed be approximated by the sum of channel capacity and flow frequency effects, and that they are within the uncertainty of the calculated trends. The

sites with the lowest discrepancy and best-fit relationship are those where the channel capacity, flow and stage time-series overlap fully (dark circles in **Figure 11**). Thus, to be able to assess the contribution of channel capacity and flow frequency effects to flood hazard precisely, it is crucial to have complete hydrologic and geomorphic data records that overlap well in space and time.

To understand how the two effects interact, we may observe the 'response' of channel geometry to changes in the flow frequency, under the premise that alluvial river channels will adjust to changes in sediment transport and hydrologic regime. Across the 41 sites, it appears that channel capacity is not adjusting significantly to flow frequency: in sites where flow frequency is increasing, there is no significant tendency for channel capacity to increase as well (to accommodate the flood flows), nor is there a significant tendency for channel capacity to decrease in response to reduced flood flows. This finding is similar to that found for the continental USA by Slater et al. (2015), even though the sample size would need to be increased to provide a more conclusive response.

Trends in flow area and mean flow velocity

Changes in channel capacity can also be broken down following equation 1 into the trend in the cross-sectional channel flow area and the trend in the mean cross-sectional flow velocity. Approximately equal proportions of sites display increasing and decreasing flow area (**Figures 12A** and **13A**), while the majority of sites reveal increasing flow velocity (**Figures 12A** and **13B**).

Comparing the magnitude of trends in cross-sectional flow area and mean flow velocity reveals that the increases in flood hazard frequency from channel capacity (red circles in **Figure 9A** where channel capacity is decreasing) are driven largely by decreases in flow area (blue circles in **Figure 13A**). Concomitantly, in many of these channels, mean flow velocity is increasing, acting as a partial counterweight to the decreases in flow area.

A small subset of the river channels exhibiting flood hazard increases due to the channel capacity effect was investigated in the Central Midlands. These sites are groundwater dominated, permeable streams, with a baseflow index (ratio of Q_{95} expressed as a percentage of Mean Annual Flow) close to 50% (e.g. Sear *et al.*, 1999). Consequently, these channels have strongly seasonal growth of macrophytes within the channel, with low to medium weed from May-June and September-October, and high weed levels in July-August. Field observations indicated very dense weed growth at the

cableway (**Figure 14**) and several hundreds of metres up and downstream of the gauging station, with visible trapping of sediment in many locations. Macrophytes growing at the gauging station location are removed several times per year, however the weed grows back at a faster rate than it is cut. **Figure 1** shows an amphibious weed cutter removing macrophytes beneath the cableway in the River Anker at Polesworth. Such heavy weed growth can lead to uncertainty in the rating curves and overestimations of the discharge that is within the channel for a given stage, so seasonal stage-discharge rating curves are sometimes employed to calibrate the measurements.

DISCUSSION

Implications of results for flood management

The 41 sites studied in this paper reveal that geomorphic trends in channel capacity can significantly alter flood hazards. These geomorphic trends, which are principally due to changes in sediment delivery, flow frequency, and vegetation growth within river channels, can be directly related to an estimated change in the flood hazard frequency. The remarkably constant relationship found at these sites (1.5 days/year increase in flood frequency for a 10% reduction in channel capacity, and vice-versa, as seen in **Figure 7**) provides some guidance for river managers who may wish to approximate the changes in flood frequency that could arise for a given change in the channel capacity. The relationship is applicable to sites with similar hydrologic regimes (i.e. similar exceedance curves) throughout England and Wales. Elsewhere, one would use the slope of the exceedance curve to determine by how much a change in the channel capacity would alter the flood frequency (**Figure 5C**). However, care should be taken in selecting flow records to estimate a channel capacity effect, due to nonstationarities in hydrologic regimes (e.g. Vogel *et al.*, 2011, Wilby and Quinn, 2013): different projected channel capacity effects may be obtained depending on the distribution of the flow that is used to compute the exceedance frequency curve (equation 7). Understanding the relationship between channel capacity and flood frequency may be of considerable use to the flood insurance industry, which has shown increasing interest in detecting geomorphic and hydrologic trends in relation to land use and land cover changes (Macklin and Harrison, 2012).

Measured flow frequency trends (**Figure 9B**) are similar to those documented in the literature across England and Wales. Although centennial time series have not revealed

any clear changes in the magnitude or frequency of flood flows (Marsh and Hannaford, 2007, Marsh and Harvey, 2012), shorter, 30- to 40- year time series, comparable to those studied here, have revealed increases, particularly in the maritime-influenced river basins across much the north and west of the UK (Robson, 2002, Hannaford and Marsh, 2008, Prodoscimi *et al.*, 2013). While these increases in flood flows are somewhat 'hard wired' in the records (Wilby and Quinn, 2013) due to the increasing North Atlantic Oscillation (NAO) index over the same period (Wilby *et al.*, 1997, Osborn *et al.*, 2000, Hulme *et al.*, 2002), future increases in flooding may also be expected as precipitation extremes become more common (Hulme *et al.*, 2002, Huntingford *et al.*, 2003), due to the greater winter rainfall totals associated with increasing temperatures (Wilby *et al.* 2008, Kay and Jones, 2012).

In this work, measured flow frequency trends outweighed the channel capacity effects on flood hazard at the majority of stations. One must however bear in mind that the comparison between the magnitude of hydrologic and geomorphic trends is slightly biased in favour of flow frequency trends because the channel cross-sectional data are measured at gauging locations, which are some of the most stable points in the fluvial network (Lamb *et al.*, 2003). Stable channel cross-sections are desirable in stream gauging since a constant rating curve is more reliable for measuring flow. However, the implication of this geomorphic stability is that any measured changes in channel geometry/capacity at cableway locations will be conservative in contrast with other locations in the landscape. It is therefore inevitable that geomorphic effects on flood hazard will be lesser than flow frequency effects in many of these locations. If channel measurements were made elsewhere, we would expect to find greater trends in channel capacity (both increases and decreases), with proportionally greater effects (*idem.*) on flood hazard. At ungauged sites, very large spatial differences have been found in channel form over periods of several years (e.g. Raven *et al.*, 2009) and over many decades (Brookes 1987, Hooke and Richmond, 1989).

Comparing the magnitude of computed trends also revealed that, for both channel capacity and flow frequency effects, the increases in flood hazard frequency tended to be more numerous and larger than the decreases (**Figure 8**). Thus, in recent years there has been a tendency for flood hazard frequency to increase from *both* geomorphic and hydrologic trends (**Figure 9**). Infilling of river channels due to weed growth (**Figure 14**) and increased sediment delivery or siltation from agriculture and other land use/land cover changes appears to be contributing to the decadal increases

in flood frequency (e.g. Lane *et al.*, 2008). These capacity changes may not be of concern in locations where flooding does not pose a threat. In farmland, for example, reductions in channel capacity may even be desirable, to allow rivers to connect with their floodplains where the water can be stored during flood events to reduce downstream flood risk. Elsewhere, however, we may wish to reconsider our approach to land use management. Natural channel capacity increases, which reduce the flood hazard by keeping streamflow within the banks, may only occur in locations where the rivers are free to adjust to increasing flows. In towns and cities where the channel is not allowed to adjust naturally, any reductions in channel capacity will certainly amplify the flood risk.

Last, this work indicates that the magnitude of the trend in flood stage frequency is typically greater than either channel capacity or flow frequency effects alone (**Figure 8**). Confounding flow frequency trends (i.e. changes in the hydrologic regime) with changes in the flood stage frequency, as is traditionally done in the literature (e.g. Milly *et al.*, 2002, Villarini *et al.*, 2009), may produce inaccurate results. Geomorphic changes in the cross-sectional flow area, mean flow velocity, channel width, or the riverbed elevation (Stover and Montgomery, 2001), measurably alter the frequency of flooding (Slater *et al.*, 2013), and the extent of their influence will vary with basinwide changes in land use, land cover, and climate, and depending on the unique qualities of individual catchments (Pattison and Lane, 2012). Further, the lack of response of channel capacity to changing flow frequency suggests that the timescales of geomorphic response may be much longer than those captured by the time-series in this analysis. While many river managers assume that the channel capacity effect is not of concern because channels eventually adjust to hydrologic change (e.g. Harvey, 1969), the case may in fact be that not all channels are able to adjust as rapidly as required, depending on their characteristics (Downs, 1995), but also if the balance between sediment and flow has been altered. Therefore, it is only by measuring these local shifts in flow area, flow velocity, and channel capacity that we may understand how flood hazard is truly changing.

Directions for future research based on hydrometric data analyses

Hydrometric archives of cross-sectional channel measurements are one of our most valuable resources for understanding how rivers are changing over time. A number of research avenues merit further investigation and are becoming increasingly practicable now that geo-referenced hydrometric measurements are gradually being published as

Open Data around the world (Dixon *et al.*, 2013). First, in order to expand these analyses to a wider number of locations, it is vital that the precise spatial reference and meta-description of each gauging transect are provided to the public along with the data. The EA are updating guidance documents on river gauging so that the exact gauging location is recorded for all gaugings (N. Everard, pers. comm.). However, the vast majority of transect measurements that have been made around the world do not contain a *precise* spatial indication of measurement location because the principal aim of gauging is to provide the most accurate measurement of the flow in the conditions present on the day, rather than to record the shape of the channel at a given point in space and time. In many hydrometric archives, the gauging measurement location is provided subjectively in a “comments” column (e.g. “measurement made 20 m upstream from bridge”). In the USA, the streamflow measurements archives from the U.S. Geological Survey (USGS)’s National water information system (NWIS) do provide a ‘Channel location code’ column with a quantified indicator to record the relative distance of the measured channel transect from the gauge, but it is seldom filled in. Automating data analyses to measure changes in channel geometry would be far easier if all hydrometric archives provided the precise coordinates of the measurements as a numeric value in a sortable column.

Finally, if all Acoustic Doppler Current Profiler (ADCP) measurements were accurately geo-located and published as Open Data online (rather than just the cross-sectional transect information, which provides average channel dimensions instead of the complete bathymetry and velocity profile), then one could conceivably automate downloads and quantify changes in river channels across a wide range of locations. An extremely worthwhile effort would be to start measuring and archiving reach-scale ADCP velocity and bathymetry measurements systematically in sensitive locations across Great Britain so that we may monitor how our rivers are changing over time, and foresee the potential effects of changing channel capacity on flood hazards.

CONCLUSION

This paper investigated the contribution of changing channel capacity to flood hazard frequency at gauging stations located across England and Wales. Trends in flood stage frequency above the 1% annual exceedance threshold were separated into the two main flood drivers that are geomorphic (channel capacity) and hydrologic (flow frequency) trends. The channel capacity effect on flood frequency was further

separated to distinguish the effects of changing area and mean velocity of the cross-sectional flow. Results indicated that positive and negative changes in channel capacity of 10% can amplify trends in flood frequency across England and Wales by ± 1.5 days per year. Both decreases and increases in flood frequency have been magnified by geomorphic changes across England and Wales. However, predicting potential future effects of changing capacity will require local studies to understand the nature of changing flow and sediment dynamics within individual channel networks. In the context of a nonstationary climate (Milly *et al.*, 2008), these findings reveal that the assumption of stationary river channels is inappropriate over short-term periods for estimating flood hazards. The adjustments and trends in channel geometry that develop over decadal timescales present a real, measurable threat to the stability of riverine infrastructure, navigation and populations.

ACKNOWLEDGMENTS

This work was partially funded by an Early Career Researcher grant to LJS from the British Society for Geomorphology (BSG Wiley-Blackwell). The Environment Agency and Natural Resources Wales are gratefully thanked for providing historic river channel transect and stage data. Streamflow time series were obtained from the National River Flow Archive (NRFA) using C. Vitolo's 'nrfa' package for the open-source software project R. The author thanks M.B. Singer and J.W. Kirchner for their guidance and support in developing many of the ideas and methods that were explored in this paper. G. Villarini is thanked for helpful comments on the manuscript, and N. Everard for providing valuable insight on stream gauging methods in England and Wales. Suggestions made by S. Lane and one anonymous reviewer are also gratefully acknowledged. The author has no conflict of interest to declare.

SUPPLEMENTARY MATERIALS

Supplementary materials contain: (1) graphs of data and of measured trends in flood stage frequency, flow frequency effects on flood hazard frequency, and channel capacity effects on flood hazard frequency; (2) graphs of data and of trends in cross-sectional flow area and mean flow velocity; (3) tables with descriptive information for each of the gauging stations, including trend length and magnitude.

BIBLIOGRAPHY

- Biedenharn, D., Watson, C. 1997. Stage adjustment in the lower Mississippi River, USA. *Regulated Rivers: Research & Management*, 13, 517–536. [http://doi.org/10.1002/\(SICI\)1099-1646\(199711/12\)13:6<517::AID-RRR482>3.0.CO;2-2](http://doi.org/10.1002/(SICI)1099-1646(199711/12)13:6<517::AID-RRR482>3.0.CO;2-2)
- Blench, T. 1969. *Mobile-bed fluviology; a regime theory treatment of canals and rivers for engineers and hydrologists*. Edmonton: University of Alberta Press.
- Brookes, A. 1987. River channel adjustments downstream from channelization works in England and Wales. *Earth Surface Processes and Landforms* 12.4: 337-351. <http://doi.org/10.1177/030913338500900103>
- Carter, R.W., Davidian, J. 1968. Chapter A6, General procedure for gaging streams, Book 3, Applications of hydraulics. In *Techniques of Water Resources Investigations of the USGS* pp. 1–13.
- Chatterton, J., Viavattene, C., Morris, J., Penning-Rowsell, E.C., Tapsell, S.M. 2010 The costs of the summer 2007 floods in England. 2010. DEFRA and Environment Agency. <http://publications.environment-agency.gov.uk/PDF/SCHO1109BRJA-E-E.pdf>
- Dixon, H., Hannaford, J., & Fry, M.J. 2013. The effective management of national hydrometric data: experiences from the United Kingdom. *Hydrological Sciences Journal*, 58(7), 1383–1399. <http://doi.org/10.1080/02626667.2013.787486>
- Downs, P.W. 1995. Estimating the Probability of River Channel Adjustment. *Earth Surface Processes and Landforms*, 20, 687–705. <http://doi.org/10.1002/esp.3290200710>
- Evans, E., Ashley, R., Saul, A., Sayers, P.B, Hall, J.W., Thorne, C., Penning-Rowsell, E.C, Watkinson, A. 2004. *Foresight future flooding: executive summary*. Office of Science and Technology, London. https://www.gov.uk/government/uploads/system/uploads/attachment_data/file/300332/04-947-flooding-summary.pdf
- Fewtrell, T.J., Neal, J.C., Bates, P.D., Harrison, P.J. 2011. Geometric and structural river channel complexity and the prediction of urban inundation. *Hydrological Processes*, 25(20), 3173–3186. <http://doi.org/10.1002/hyp.8035>
- Gilbert, G.K. 1917. *Hydraulic-mining debris in the Sierra Nevada*. No 105. Menlo Park, CA: US Government Printing Office.
- Hall, J., Sayers, P., Dawson, R. 2005. National-scale assessment of current and future flood risk in England and Wales. *Natural Hazards*, 36(1-2), 147–164. <http://doi.org/10.1007/s11069-004-4546-7>

- Hall, J.W., Evans, E.P., Penning-Rowsell, E.C., Sayers, P.B., Thorne, C.R., Saul, A.J. 2003. Quantified scenarios analysis of drivers and impacts of changing flood risk in England and Wales: 2030–2100. *Environmental Hazards*, 5(3-4), 51–65. <http://doi.org/10.1016/j.hazards.2004.04.002>
- Hannaford, J., Marsh, T. 2008. High-flow and flood trends in a network of undisturbed catchments in the UK. *International Journal of Climatology*, 1338, 1325–1338. <http://doi.org/10.1002/joc>
- Harvey, A.M. 1969. Channel capacity and the adjustment of streams to hydrologic regime. *Journal of Hydrology*, 8, 82–98.
- Helsel, D.R., Hirsch, R.M. 1993. Chapter A3 - Statistical Methods in Water Resources, Book 4 - Hydrologic Analysis and Interpretation. In *Techniques of Water Resources Investigations of the United States Geological Survey* (Vol. 36, pp. 1–510). Amsterdam: Elsevier. <http://doi.org/10.2307/1269385>
- Herschey, R.W. 1995. *Streamflow Measurement*, CRC Press, p. 486.
- Hooke J.M., Redmond C.E. 1989. River-Channel Changes in England and Wales. *Water and Environment Journal* 3: 328–335. <http://doi.org/10.1111/j.1747-6593.1989.tb01537.x>
- Hooke, J.M., Brookes, C.J., Duane, W., Mant, J.M. 2005. A simulation model of morphological, vegetation and sediment changes in ephemeral streams. *Earth Surface Processes and Landforms*, 30(7), 845–866. <http://doi.org/10.1002/esp.1195>
- Hulme, M., Jenkins, G.J., Lu, X., Turnpenny, J.R., Mitchell, T.D., Jones, R.G., Lowe, J., Murphy, J.M., Hassell, D., Boorman, P., McDonald, R. Hill, S. 2002. *Climate Change Scenarios for the United Kingdom: the UKCIP02 Scientific Report*, Tyndall Centre, University of East Anglia, Norwich.
- Huntingford, C., Jones, R.G., Prudhomme, C., Lamb, R., Gash, J.H.C., Jones, D.A. 2003. Regional climate-model predictions of extreme rainfall for a changing climate. *Quarterly Journal of the Royal Meteorological Society*, 129(590), 1607–1621. <http://doi.org/10.1256/qj.02.97>
- Huntingford, C., Marsh, T., Scaife, A., Kendon, E.J., Hannaford, J., Kay, A.L., Lockwood, M., Prudhomme, C., Reynard, N.S., Parry, S., Lowe, J.A., Screen, J., Ward, H.C., Roberts, M., Stott, P., Bell, V., Bailey, M., Jenkins, A., Legg, T., Otto, F.E.L., Massey, N., Schaller, N., Slingo, J., Allen, M.R. 2014. Potential influences on the United Kingdom's floods of winter 2013/14. *Nature Climate Change*, 4(9), 769–777. <http://doi.org/10.1038/nclimate2314>
- James, L.A. 1991. Incision and morphologic evolution of an alluvial channel recovering from hydraulic mining sediment. *Geological Society of America Bulletin*, 103(6), 723–736. [http://doi.org/10.1130/0016-7606\(1991\)103<0723](http://doi.org/10.1130/0016-7606(1991)103<0723)

- James, L.A. 1997. Channel incision on the Lower American River, California, from streamflow gage records. *Water Resources Research*, 33(3), 485–490. <http://doi.org/10.1029/96WR03685>
- Kay, A. L., Jones, D.A. 2012. Transient changes in flood frequency and timing in Britain under potential projections of climate change. *International Journal of Climatology*, 32(4), 489–502. <http://doi.org/10.1002/joc.2288>
- Kjeldsen, T.R. 2010. Modelling the impact of urbanization on flood frequency relationships in the UK. *Hydrology. Research*, 41,5 391–405, <http://doi.org/10.2166/nh.2010.056>
- Lamb R., Zaidman, M.D., Archer, D.R. Marsh, T.J., Lees, M.L., 2003. River Gauging Station Data Quality Classification, R&D Technical Report W6-058/TR. Environment Agency. https://www.gov.uk/government/uploads/system/uploads/attachment_data/file/290629/sw6-058-tr-e-e.pdf
- Lane, S. N., Tayefi, V., Reid, S., Yu, D., Hardy, R. 2007. Interactions between sediment delivery, channel change, climate change and flood risk in a temperate upland environment. *Earth Surface Processes and Landforms*, 32(3), 429–446. <http://doi.org/10.1002/esp>
- Lang, M., Ouarda, T.B.M.J., Bobée, B. 1999. Towards operational guidelines for over-threshold modeling. *Journal of Hydrology*, 225(3-4), 103–117. [http://doi.org/10.1016/S0022-1694\(99\)00167-5](http://doi.org/10.1016/S0022-1694(99)00167-5)
- Leopold, L. B., & Maddock, T. (1953). The Hydraulic Geometry of Stream Channels and Some Physiographic Implications. U.S. Geological Survey Professional Paper, 252, 1–57.
- Macklin, M., Harrison, S. 2012. Geomorphology and changing flood risk in the UK, Climate Change Risk Management Ltd for Lloyd's. http://www.lloyds.com/~media/Files/The%20Market/Tools%20and%20resources/Exposure%20management/20120402Geomorphology_report.pdf
- Marsh, T.J., Harvey, C.L. 2012. The Thames flood series: a lack of trend in flood magnitude and a decline in maximum levels. *Hydrology Research* Vol. 43(3). <http://doi.org/10.2166/nh.2012.054>
- Marsh, T.J., Hannaford, J. 2007. The summer 2007 floods in England and Wales – a hydrological appraisal. Centre for Ecology & Hydrology. 32pp.
- Marsh, T.J., Harvey, C.L. 2012. The Thames flood series: a lack of trend in flood magnitude and a decline in maximum levels. *Hydrology Research*, 43.3 203–214, <http://doi.org/10.2166/nh.2012.054>
- Milly, P.C.D., Wetherald, R.T., Dunne, K.A., Delworth, T.L. 2002. Increasing risk of great floods in a changing climate. *Nature* 415: 514–517: <http://doi.org/10.1038/415514a>

- Milly, P.C.D., Betancourt, J., Falkenmark, M., Hirsch, R.M., Kundzewicz, Z.W., Lettenmaier, D.P., & Stouffer, R. 2008. Stationarity is dead: whither water management? *Science* (New York, N.Y.), 319(5863), 573–574. <http://doi.org/10.1126/science.1151915>
- Naden, P.S., 1992. Analysis and use of peaks-over-threshold data in flood estimation. In: Saul, A.J., (Ed.), *Floods and Flood Management*, Kluwer, Dordrecht, pp. 131–143.
- Neuhold, C., Stanzel, P., Nachtnebel, H.P. 2009. Incorporating river morphological changes to flood risk assessment: uncertainties, methodology and application. *Natural Hazards and Earth System Science*, 9(3), 789–799. <http://doi.org/10.5194/nhess-9-789-2009>
- Osborn, T.J., Hulme, M., Jones, P.D., Basnett, T.A. 2000. Observed trends in the daily intensity of United Kingdom precipitation. *International Journal of Climatology*, 20(4), 347–364. [http://doi.org/10.1002/\(SICI\)1097-0088\(20000330\)20:4<347::AID-JOC475>3.0.CO;2-C](http://doi.org/10.1002/(SICI)1097-0088(20000330)20:4<347::AID-JOC475>3.0.CO;2-C)
- Pall, P., Aina, T., Stone, D.A., Stott, P.A., Nozawa, T., Hilberts, A.G.J., Lohmann, D. Allen, M.R. 2011. Anthropogenic greenhouse gas contribution to flood risk in England and Wales in autumn 2000. *Nature*, 470(7334), 382–385. <http://doi.org/10.1038/nature09762>
- Pattison, I., Lane, S. N. 2012. The link between land-use management and fluvial flood risk: A chaotic conception? *Progress in Physical Geography*, 36(1), 72–92. <http://doi.org/10.1177/0309133311425398>
- Pinter, N., Heine, R.A. 2005. Hydrodynamic and morphodynamic response to river engineering documented by fixed-discharge analysis, Lower Missouri River, USA. *Journal of Hydrology*, 302(1-4), 70–91. <http://doi.org/10.1016/j.jhydrol.2004.06.039>
- Prosdoci, I., Kjeldsen, T.R., Svensson, C. 2013. Non-stationarity in annual and seasonal series of peak flow and precipitation in the UK. *Natural Hazards and Earth System Sciences Discussions*, 1(5), 5499–5544. <http://doi.org/10.5194/nhessd-1-5499-2013>
- Prosdoci, I., Kjeldsen, T.R., Miller, J.D. 2015. Detection and attribution of urbanization effect on flood extremes using nonstationary flood-frequency models. *Water Resources Research*, 1–19. <http://doi.org/10.1002/2015WR017065>
- Raven, E., Lane, S.N., Ferguson, R. 2009. The spatial and temporal patterns of aggradation in a temperate, upland, gravel bed river. *Earth Surface Processes and Landforms*, 1197(34), 1181–1197. <http://doi.org/10.1002/Esp.1783>
- Robson, A.J. 2002. Evidence for trends in UK flooding. *Philosophical Transactions of the Royal Society. Series A, Mathematical, Physical, and Engineering Sciences*, 360(1796), 1327–43. <http://doi.org/10.1098/rsta.2002.1003>
- Schumm, S.A., Lichty, R. 1965. Time, space, and causality in geomorphology. *American Journal of Science*, 263(2), 110–119. <http://doi.org/10.2475/ajs.263.2.110>

- Sear, D.A., Armitage, P.D., Dawson, F.H. 1999. Groundwater dominated rivers. *Hydrological Processes*, 13(3), 255–276. [http://doi.org/10.1002/\(SICI\)1099-1085\(19990228\)13:3<255::AID-HYP737>3.0.CO;2-Y](http://doi.org/10.1002/(SICI)1099-1085(19990228)13:3<255::AID-HYP737>3.0.CO;2-Y)
- Simpson, I. R., Jones P.D. 2014. Analysis of UK precipitation extremes derived from Met Office gridded data. *International Journal of Climatology* 34.7: 2438-2449.
- Slater, L.J., Singer, M.B. 2013. Imprint of climate and climate change in alluvial riverbeds: Continental United States, 1950-2011. *Geology*, 41(5), 595–598. <http://doi.org/10.1130/G34070.1>
- Slater, L.J., Singer, M.B., Kirchner, J.W. 2015. Hydrologic versus geomorphic drivers of trends in flood hazard. *Geophysical Research Letters*, 42, 1–7. <http://doi.org/10.1002/2014GL062482>
- Slingo, J., Belcher S., Scaife A., McCarthy, M., Saulter, A., McBeath, K., Jenkins A., Huntingford, C., Marsh, T., Hannaford J., Parry, S. 2014. The recent storms and floods in the UK. Met Office, Centre for Ecology & Hydrology. http://www.metoffice.gov.uk/media/pdf/n/i/Recent_Storms_Briefing_Final_07023.pdf
- Stover, S., Montgomery, D.R. 2001. Channel change and flooding, Skokomish River, Washington. *Journal of Hydrology*, 243(3-4), 272–286. [http://doi.org/10.1016/S0022-1694\(00\)00421-2](http://doi.org/10.1016/S0022-1694(00)00421-2)
- Thorne, C. 2014. Geographies of UK flooding in 2013/4. *The Geographical Journal*, 180(4), 297–309. <http://doi.org/10.1111/geoj.12122>
- Villarini, G., Smith J.A., Serinaldi F., Bales J., Bates P.D., Krajewski, W.F. 2009. Flood frequency analysis for nonstationary annual peak records in an urban drainage basin. *Advances in Water Resources*, 32(8), 1255–1266. <http://doi.org/10.1016/j.advwatres.2009.05.003>
- Vitolo C., Fry M. 2014. RNRFA, R package, National River Flow Archive, GitHub repository, <http://dx.doi.org/10.5281/zenodo.14722> https://github.com/cvitolo/r_rnrfa
- Vogel, R.M., Yaindl C., Walter M. 2011. Nonstationarity: Flood Magnification and Recurrence Reduction Factors in the United States, *Journal of American Water Resources Association*, 47(3):464-474. <http://doi.org/10.1111/j.1752-1688.2011.00541.x>.
- Wheater, H., Evans E. 2009. Land use, water management and future flood risk. *Land Use Policy*, 26, 251–264. <http://doi.org/10.1016/j.landusepol.2009.08.019>
- Wilby, R.L., O'Hare, G., Barnsley, N., 1997. The North Atlantic Oscillation and British Isles climate variability 1865–1995. *Weather*, 52(9), 266–276. <http://doi.org/10.1002/j.1477-8696.1997.tb06323.x>

- Accepted Article
- Wilby, R.L. 2006. When and where might climate change be detectable in UK river flows? *Geophysical Research Letters*, 33, L19407, <http://doi.org/10.1029/2006GL027552>
- Wilby, R. L., Beven, K. J., Reynard, N. S. 2008. Climate change and fluvial flood risk in the UK: more of the same? *Hydrological Processes*, 22, 2511–2523. <http://doi.org/10.1002/hyp>
- Wilby, R.L., Quinn, N.W. 2013. Reconstructing multi-decadal variations in fluvial flood risk using atmospheric circulation patterns. *Journal of Hydrology*, 487, 109–121. <http://doi.org/10.1016/j.jhydrol.2013.02.038>
- Wong, J.S., Freer J.E., Bates P.D., Sear D.A., Stephens, E.M. 2014. Sensitivity of a hydraulic model to channel erosion uncertainty during extreme flooding. *Hydrological Processes*, 1–19. <http://doi.org/10.1002/hyp.10148>

River Tawe at Ynystanglws



River Anker at Polesworth



River Dove at Marston on Dove



River Tame at Hopwas Bridge



River Trent



Figure 1. Photographs of cableway gauging stations in Wales (River Tawe) and in the Central Midlands (Rivers Anker, Dove, Tame, and Trent). The cableway location is presented in each photograph, although not always visible. An amphibious weed cutter labelled “a” can be seen in the River Anker under the cableway.

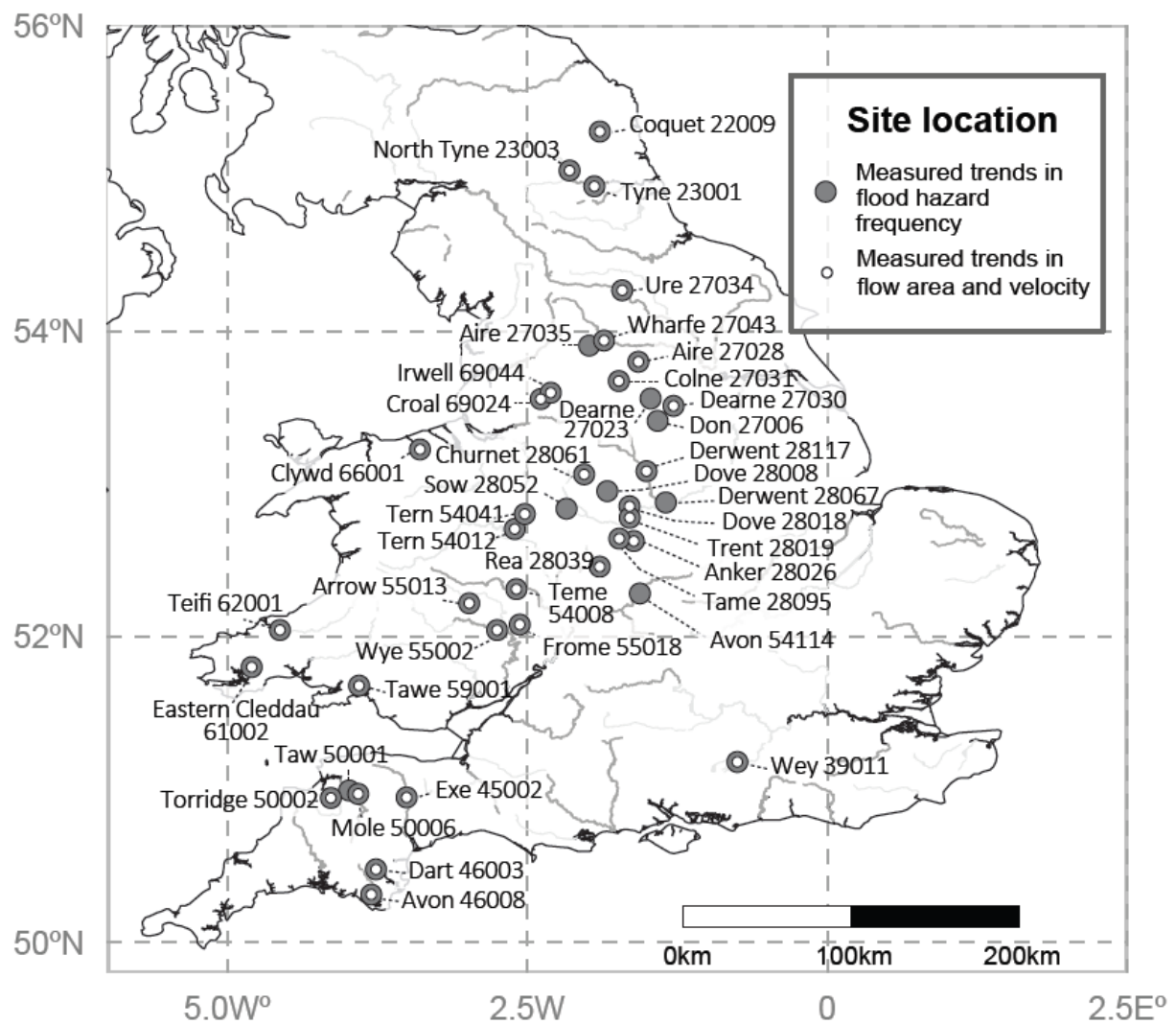


Figure 2. Location map of the 41 channel cross-sections where trends in the channel capacity effect on flood hazard, the flow frequency effect on flood hazard, and the flood stage frequency were computed (grey circles). At 34 of those sites (white inner circles), trends in the cross-sectional channel flow area and mean flow velocity were also investigated.

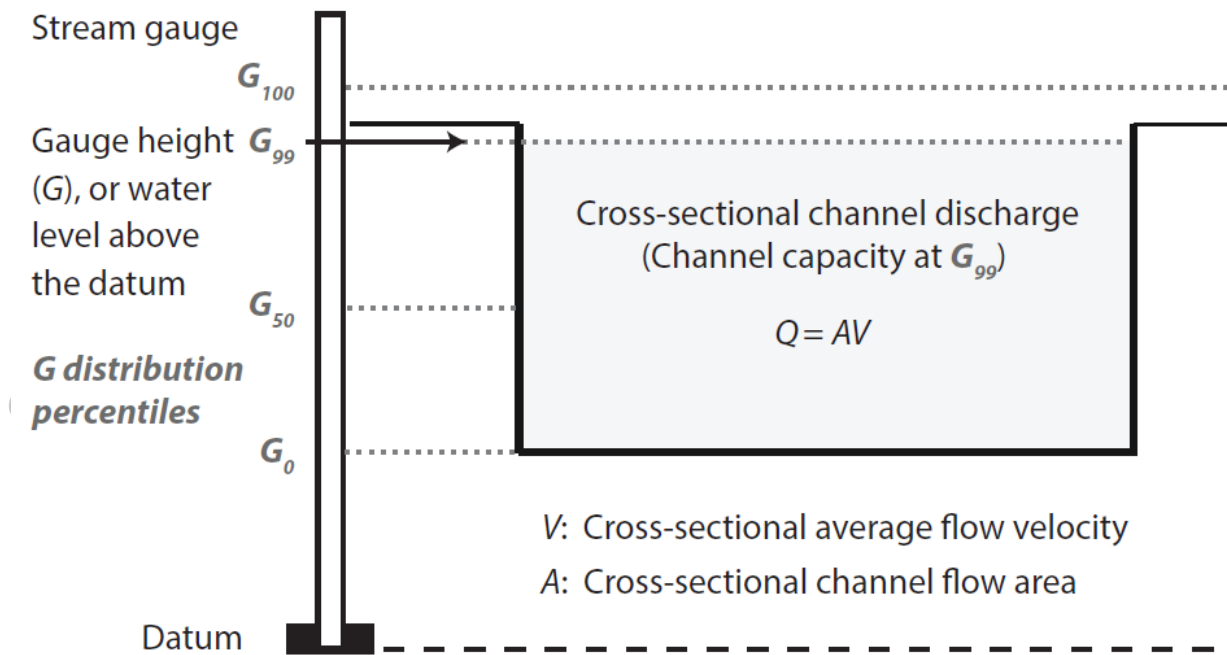


Figure 3. Schematic channel cross-section indicating cross-sectional discharge (Q), cross-sectional flow area (A) and cross-sectional average flow velocity (V), with different values of stage (G), indicated by dotted horizontal lines. Gauging transect measurements are generally made for the full range of stage (at both low and high-flow conditions) to obtain a complete stage-discharge rating curve. The exact distribution of stage percentiles, suggested by the dotted lines, varies with each gauging site depending on site-specific factors such as the shape of the channel cross-section and flow regime. G_{50} indicates the median value of the stage distribution, and G_{99} the 99th percentile.

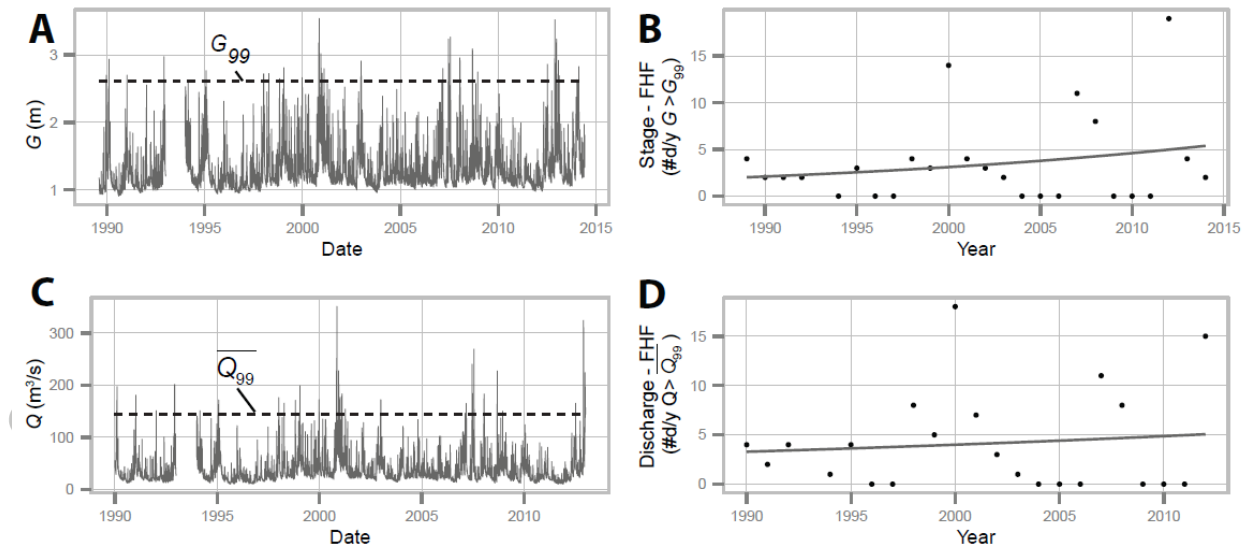


Figure 4. Computing the trend in flood stage frequency (top panels) and the flow frequency effect on flood hazard (bottom panels) at the River Trent near Drakelow, NRFA site number 28019 (same site in Figures 1, 4-6 and 14). A) Stage hydrograph. Dashed horizontal black line indicates the 99th percentile of the stage distribution (G_{99}). B) Trend in total number of days per year where stage exceeded G_{99} . C) Discharge hydrograph. Dashed horizontal black line indicates the time-averaged channel capacity at G_{99} (Q_{99} , see Figure 3A). D) Trend in total number of days per year where discharge exceeded Q_{99} . Complete trends are for all sites are provided in the supplementary materials.

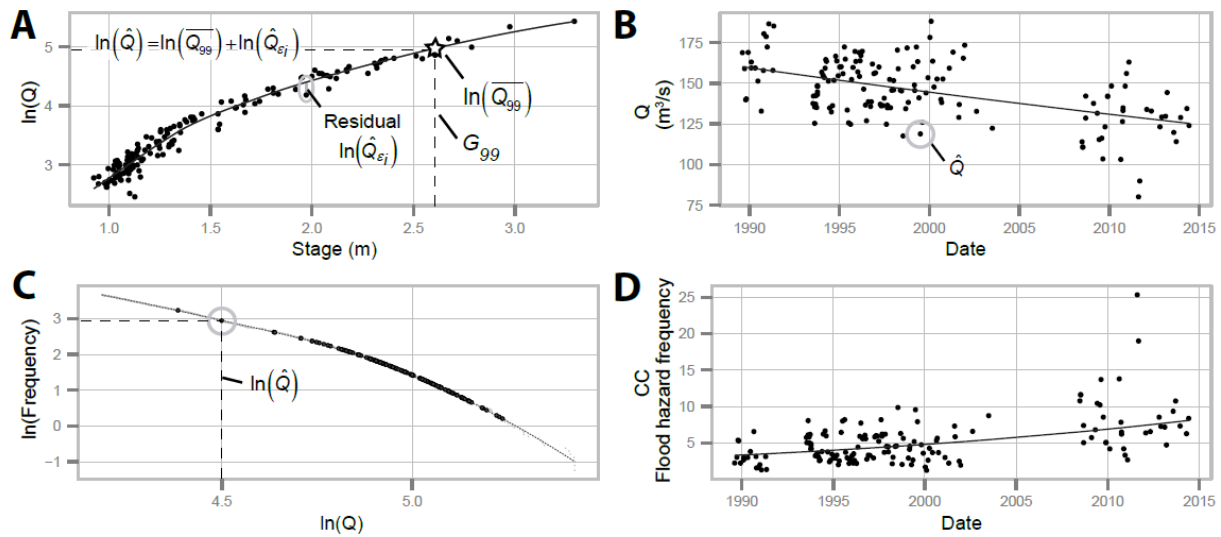


Figure 5. Computing the channel capacity effect, or the trend in flood hazard frequency that is due to geomorphic changes in channel capacity, for the River Trent near Drakelow (same site in Figures 1, 4-6 and 14). A) Relationship between Stage (G) and the natural log of Discharge ($\ln(Q)$). Black circles represent channel transect measurements collected at different points in time. The Locally Weighted Scatterplot Smoothing (Loess) curve passing through the measurements is shown in black. The time-averaged channel capacity at G_{99} in log form, $\ln(\bar{Q}_{99})$, is extracted at the point where the Loess curve intersects with G_{99} . Residuals are measured as the vertical distance between each black circle and the Loess rating curve, and indicate how each measurement deviates from the average value on the curve, for the corresponding stage. Channel capacity is estimated (in log form, $\ln(\hat{Q})$) at the time of each transect measurement, as the sum of $\ln(\bar{Q}_{99})$ and each residual from the curve, $\ln(\hat{Q}_{99})$. B) Trend in estimated channel capacity at G_{99} over time. C) An exceedance frequency curve is computed over the same period during which the channel measurements were made, using the daily discharge data (same data as in Figure 4C). Black circles indicate $\ln(\hat{Q})$, i.e. logged estimates of the channel capacity at G_{99} at different points in time. A Loess curve is fit through the exceedance curve to smooth any variability (grey line) and exceedance frequencies are extracted where $\ln(\hat{Q})$ values intersect with the curve. Note that only mean daily streamflow values within a range of ± 0.2 log units above or below the $\ln(\hat{Q})$ values are used, to obtain a close fit of the Loess curve. D) Trend in estimated exceedance frequencies for the channel capacity (the values obtained in panel C are back-transformed before they are plotted in panel D). Trends are provided for all sites in the supplementary materials.

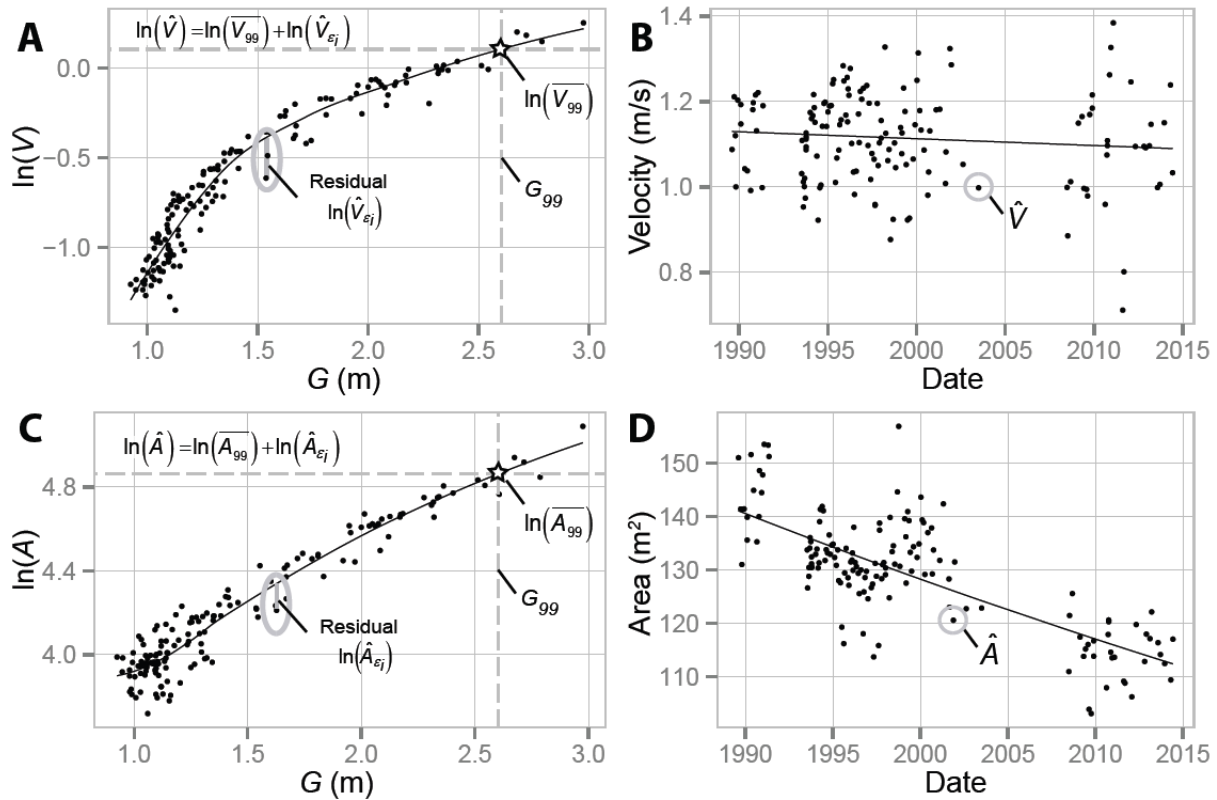


Figure 6. Computing trends in cross-sectional mean flow velocity (V), and flow area (A), River Trent near Drakelow (same site in Figures 1, 4-6 and 14). A and C), Relationship between Stage (G) and the log-transformed measurements of V and A . Black circles represent channel transect measurements collected at different points in time. Black Loess curves are shown passing through the data points. The time-averaged cross-sectional mean flow velocity and flow area in log form, $\ln(\overline{V_{99}})$ and $\ln(\overline{A_{99}})$, are extracted at the point where the Loess curves intersect with G_{99} . Residuals are measured as the vertical distance between each black circle and the Loess rating curve, and indicate how each measurement deviates from the average value on the Loess rating curve, for the corresponding stage. Cross-sectional V and A at G_{99} are estimated (in log form) at the time of each transect measurement as the sum of $\ln(\overline{V_{99}})$ or $\ln(\overline{A_{99}})$ and each individual residual. In panels B and D, black curves indicate the temporal trends in the estimated values of \hat{V} and \hat{A} , respectively. Note: the curves are exponential, but the curvature is indistinct for many sites due to the scatter in the underlying data. Trends are provided for all sites in the supplementary materials.

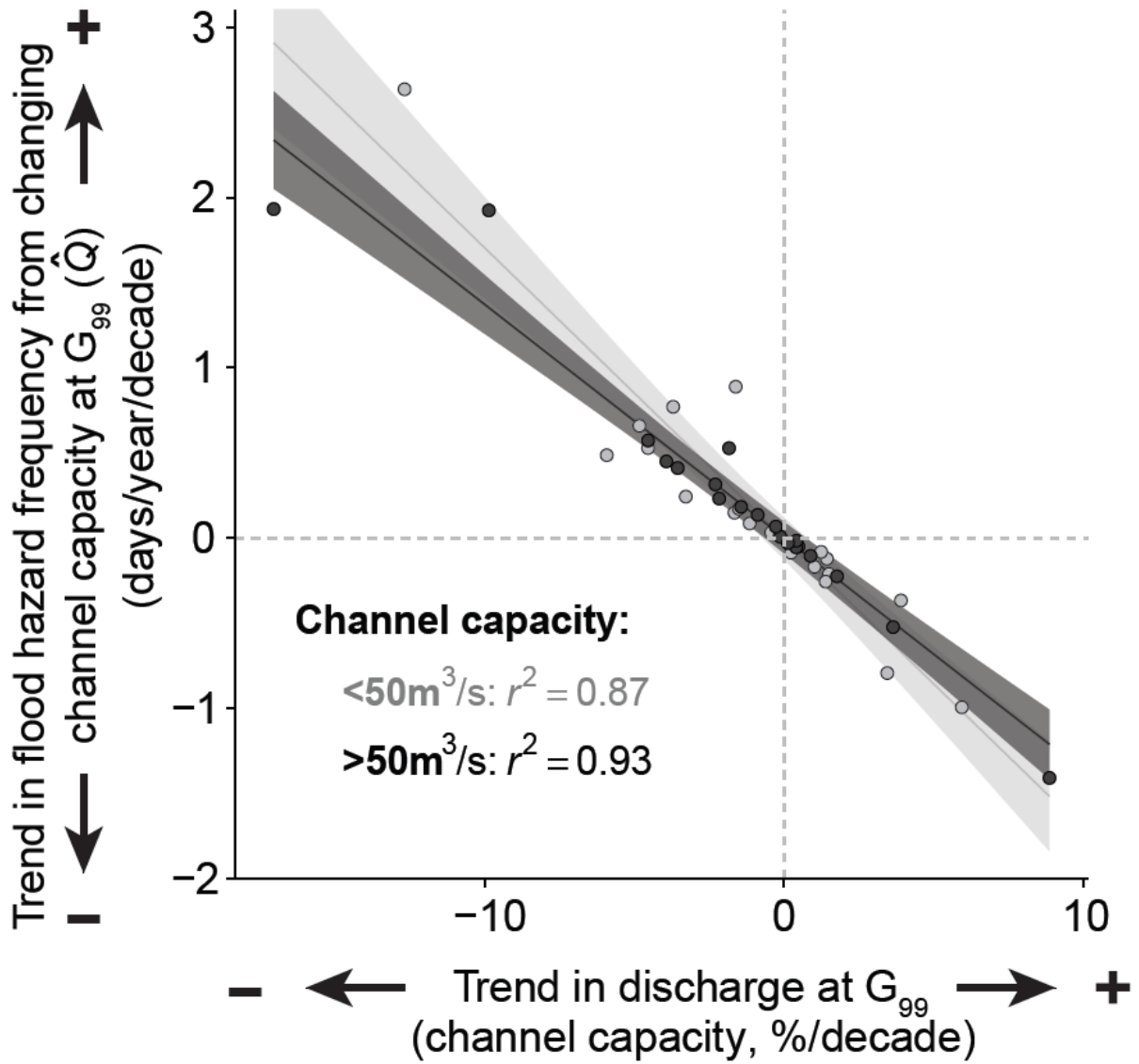


Figure 7. Relationship between the trend in channel ‘capacity’ (estimated cross-sectional discharge at Q_{99} , i.e. \hat{Q} , in %/decade) and the resulting trend in flood hazard frequency (in days/year/decade). A threshold value of $50\text{m}^3/\text{s}$ was chosen for separating small and large channels, to obtain a similar number of sites in both categories.

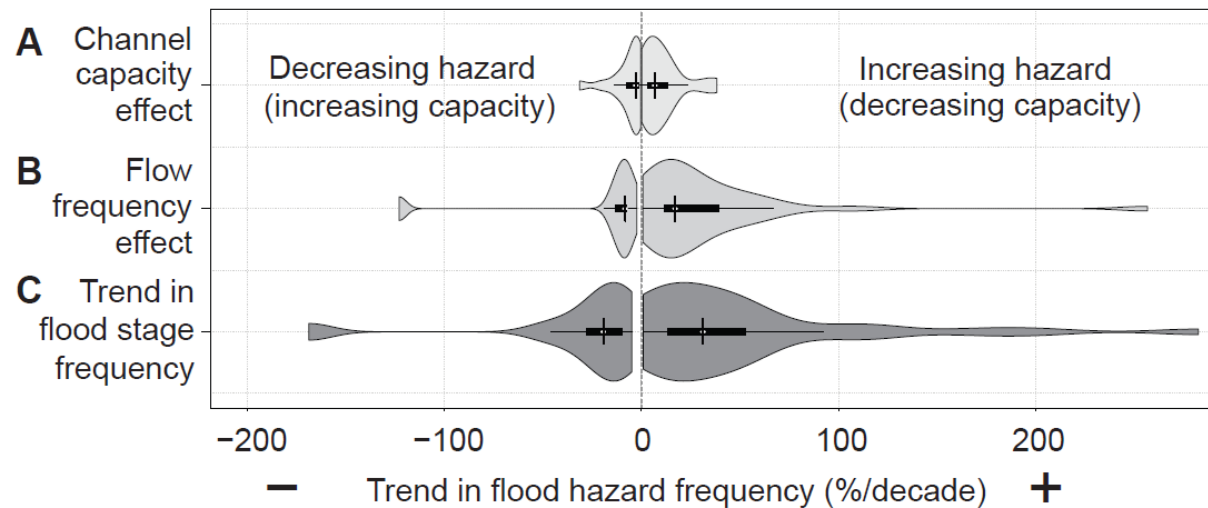


Figure 8. Trends in (A) the channel capacity effect on flood hazard, (B) the flow frequency effect on flood hazard, and (C) flood stage frequency (total flood hazard frequency). Three violin plots indicate the distribution of the 41 computed trends in flood hazard frequency, separated by their sign (positive/negative). Violins are composed of a standard black boxplot with a rotated kernel density plot on either side. Trends are shown in percent per decade, so they are directly comparable. Median of the positive/negative distributions is indicated by the short vertical black line in the centre of each violin. The trend in flood stage frequency is the result of both channel capacity and flow frequency effects, which may be positive or negative.

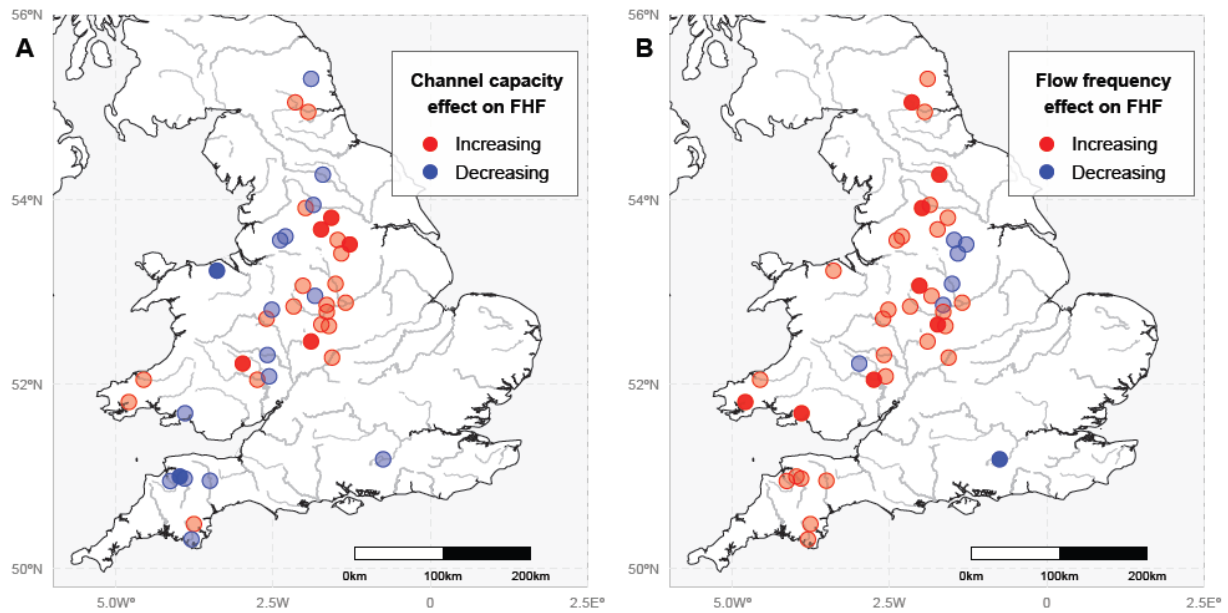


Figure 9. Maps of trends in flood hazard frequency (FHF) due to the channel capacity effect and the flow frequency effect. Red circles indicate increases in flood hazard frequency due to decreasing channel capacity (A) and increased frequency of flood flows (B). Blue circles indicate decreases in flood hazard frequency due to increasing channel capacity (A) and decreased frequency of flood flows (B).

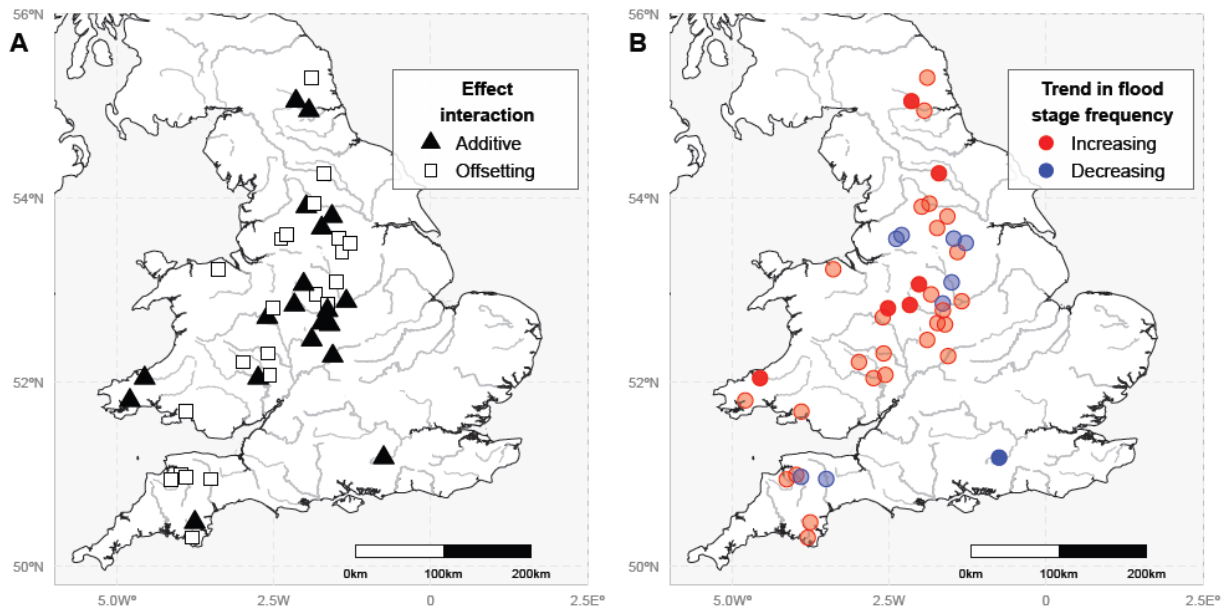


Figure 10. Interaction between channel capacity and flow frequency effects, and the resulting trend in flood stage frequency. A) Direction of the interaction between channel capacity and flow frequency effects. Additive sites indicate locations where channel capacity and flow frequency have the same, cumulative effect on flood hazard (increasing together, or decreasing together). Offsetting sites (open white squares) indicate sites where the two effects are behaving in an opposite manner, therefore attenuating the total change in flood hazard frequency. B) Trend in flood stage frequency, i.e. total change in flood hazard, resulting from the combination of these two effects.

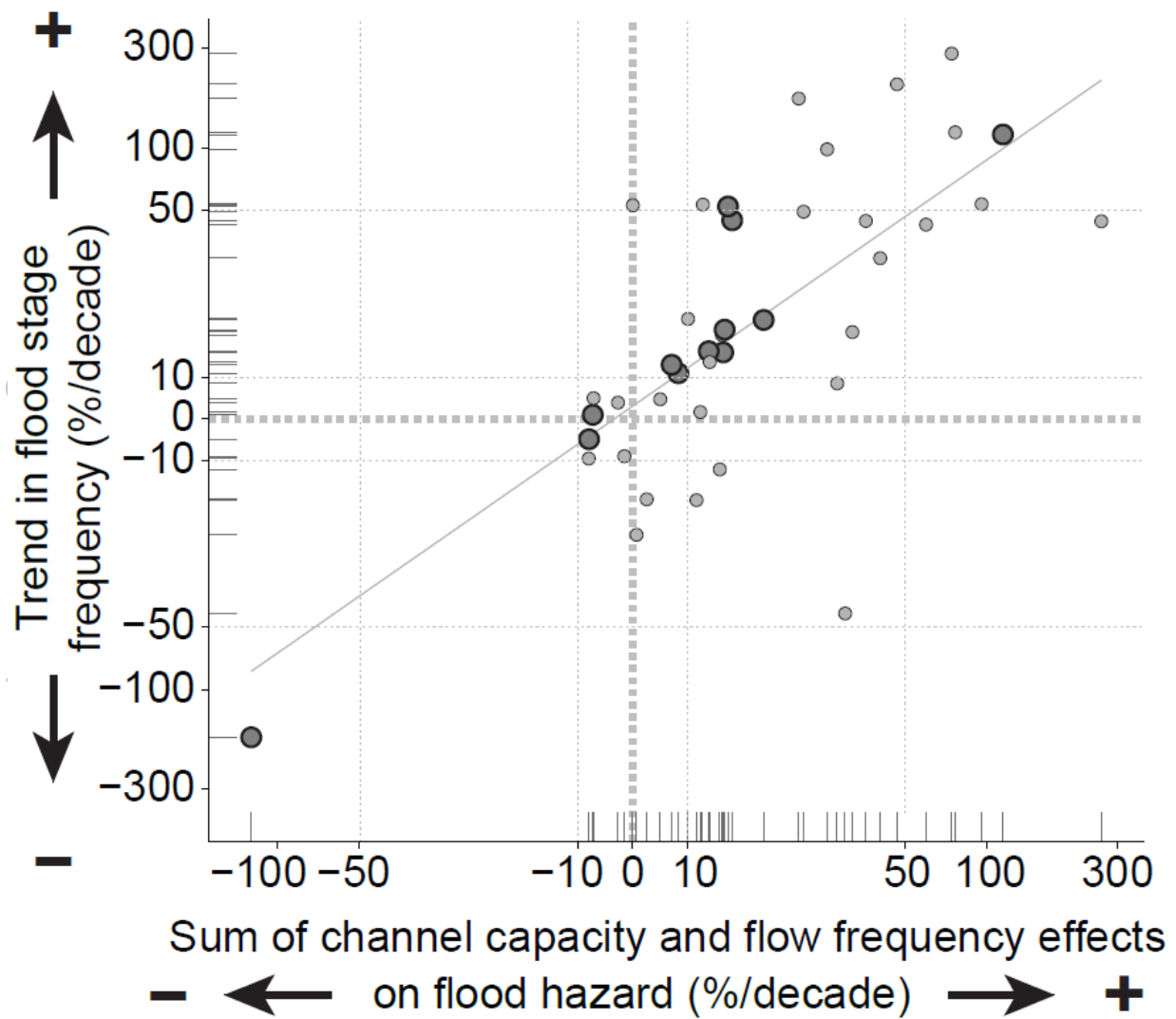


Figure 11. Relationship between the sum of channel capacity and flow frequency effects (in %/decade) and the total change in flood hazard as measured by the trend in flood stage frequency (also in %/decade). The Spearman's rank correlation coefficient for these data is 0.690, p -value<0.001. Large dark circles indicate gauging stations where the channel capacity effect, the flow frequency effect and the flood stage frequency time series overlap entirely. Axes are plotted logarithmically above the value of 50% per decade to accommodate the leptokurtic shape of the distribution (the majority of points are clustered between $\pm 50\%$, as seen in Figure 8).

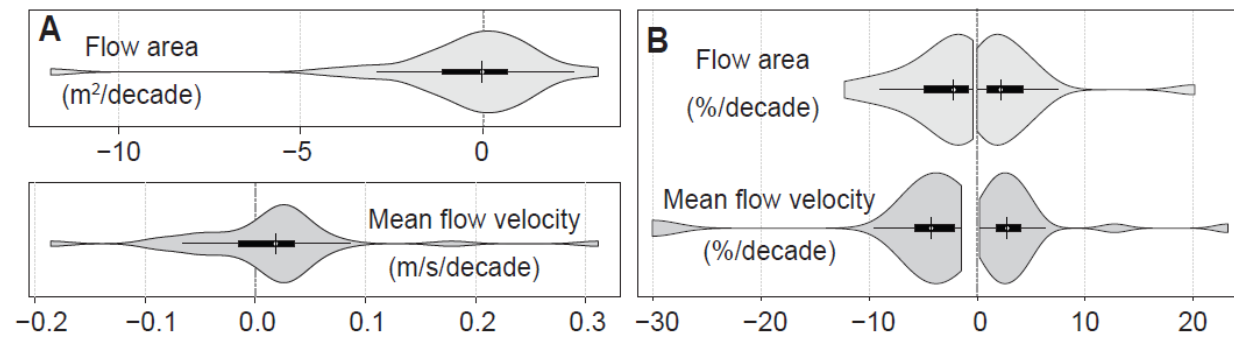


Figure 12. Distribution of trends in the cross-sectional flow area and mean cross-sectional flow velocity at each site. A) Dimensional trends in flow area (m^2/decade) and mean flow velocity (m/s/decade) are provided for scale. B) Percentage trends in the same variables are split into positive and negative trends to highlight their median magnitudes separately. Symbology is the same as in Figure 8.

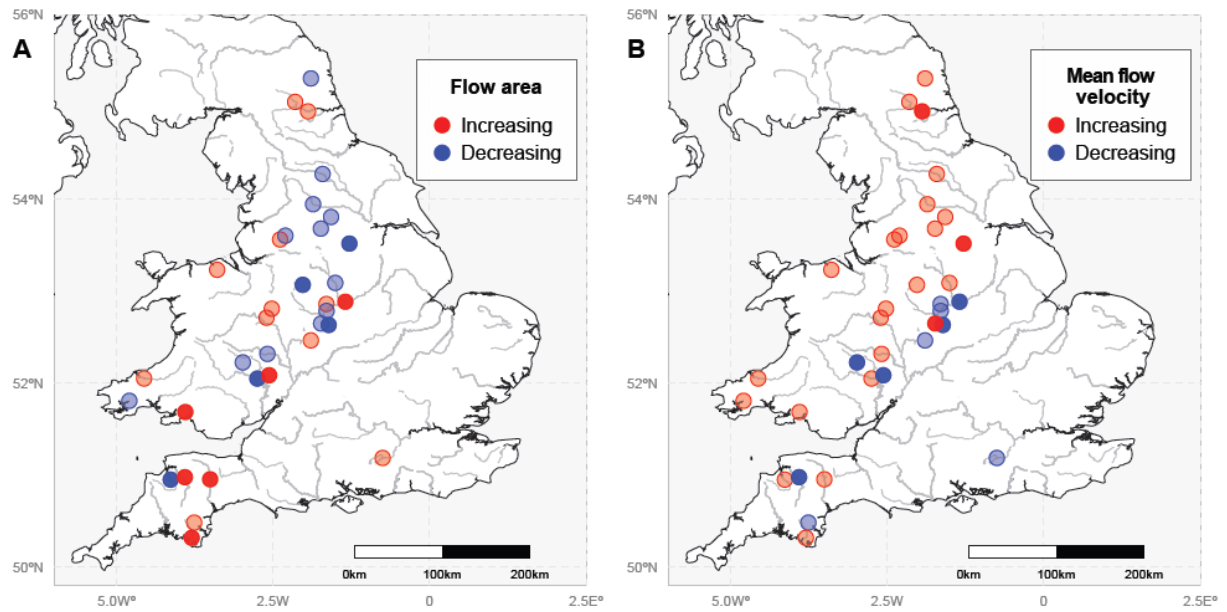


Figure 13. Trends in the flow area (A) and mean flow velocity (B) of river channel cross-sections. Red circles indicate increasing flow area and flow velocity (increasing the channel capacity) and blue circles indicate decreasing flow area and flow velocity (decreasing the channel capacity). Significant trends are indicated as solid colours and non-significant trends as transparent colours.

River Trent at Drakelow



River Tame at Hopwas Bridge



River Anker at Polesworth



Figure 14. Photographs of weeds growing within the river channels in the Central Midlands, June 2015.